Exploring the synergetic effects of the major components of biomass additives in the pyrolysis of polylactic acid

Ce Sun[1], Xiaojian Chen[1], Dingyuan Zheng[1], Wenrui Yao[1], Haiyan Tan[1], Yanhua Zhang*[1], Song Liu*[2]

[1]Key Laboratory of Bio-based Material Science & Technology, Northeast Forestry University, Ministry of Education, Harbin 150040, China

[2] College of Chemistry, Chemical Engineering and Resource Utilization, Northeast Forestry University, Harbin 150040, China

* Co-corresponding author: **Yanhua Zhang:** zhangyanhua@nefu.edu.cn;

Song Liu: carlosliusong@nefu.edu.cn

S1. Materials and methods

S1.1 Raman spectrometer

The molecular structure of the pyrolysis char was determined by a DXR2xi Raman microscopic imaging spectrometer (Thermo Fisher Scientific Co., Ltd) with 532 nm excitation wavelength at 6.8 mW power at 120 Hz. The spectrum range was from 500-4000 cm^{-1} with 900 scans per sample.

S1.2 X-ray photoelectron spectroscopy (XPS)

The element of the pyrolysis char was investigated by (Thermo Fisher Scientific Co., Ltd). Monochromatic Al Kα radiation (1486.6 eV) with resolution of Ag 3d 0.8 eV was used to make analysis.

S1.3 Pyrolysis experiments

A sample of 1g was added to the quartz tube of the pyrolysis furnace, and the temperature was raised from room temperature to 500°C at a heating rate of 10°C/min. The volatile substances generated by the reaction were passed into the formaldehyde collection tube for condensation and collection

S1.4 Kinetic analysis

Table S1. Differential and integral equations for different solid-state reaction mechanisms during decomposition processes.

Symbol	Reaction mechanisms	$f(\alpha) = (1/k)(d\alpha/dt)$	$g(\alpha) = kt$

Reaction order			
F1	First-order	$1-\alpha$	$-ln(1-\alpha)$
F1.5	1.5th-order	$(1-\alpha)^{3/2}$	$2[(1-\alpha)^{-1/2}-1]$
F2	Second-order	$(1-\alpha)^{2}$	$2(1-\alpha)^{-1}-1$
F3	Third-order	$(1-\alpha)^{3}$	$[(1-\alpha)^{-2}-1]/2$
F4	Fourth-order	$(1-\alpha)^{4}$	$[(1-\alpha)^{-3}-1]/3$
A2	Avrami-Erofeev	$2(1-\alpha)[-ln(1-\alpha)]^{1}$	$[-ln(1-\alpha)]^{1/2}$
A3	Avrami-Erofeev	$3(1-\alpha)[-ln(1-\alpha)]^{2}$	$[-ln(1-\alpha)]^{1/3}$
A4	Avrami-Erofeev	$4(1-\alpha)[-ln(1-\alpha)]^{3}$	$[-ln(1-\alpha)]^{1/4}$
Contracting geometry			
R2	Contracting cylinder	$2(1-\alpha)^{1/2}$	$1-(1-\alpha)^{1/2}$
R3	Contracting sphere	$3(1-\alpha)^{3/2}$	$1-(1-\alpha)^{1/3}$
Diffusional			
D1	One-dimensional diffusion	$1/2\alpha$	α^{2}
D2	Two-dimensional diffusion (Valensi)	$[-ln(1-\alpha)]^{-1}$	$(1-\alpha)\ln(1-\alpha)+\alpha$

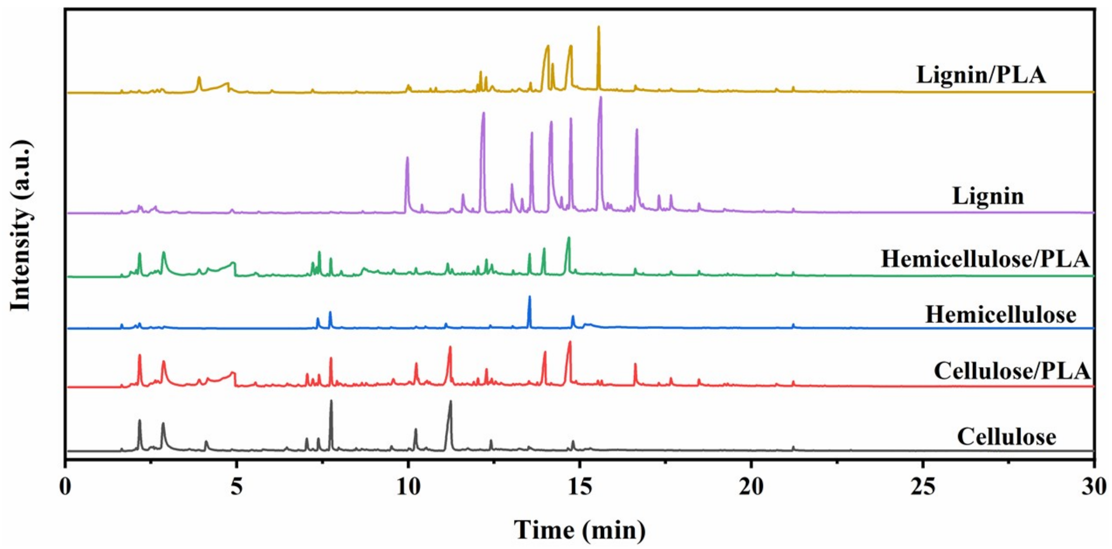

Fig. S1 The Ion map of pyrolysis products using Py-GC/MS

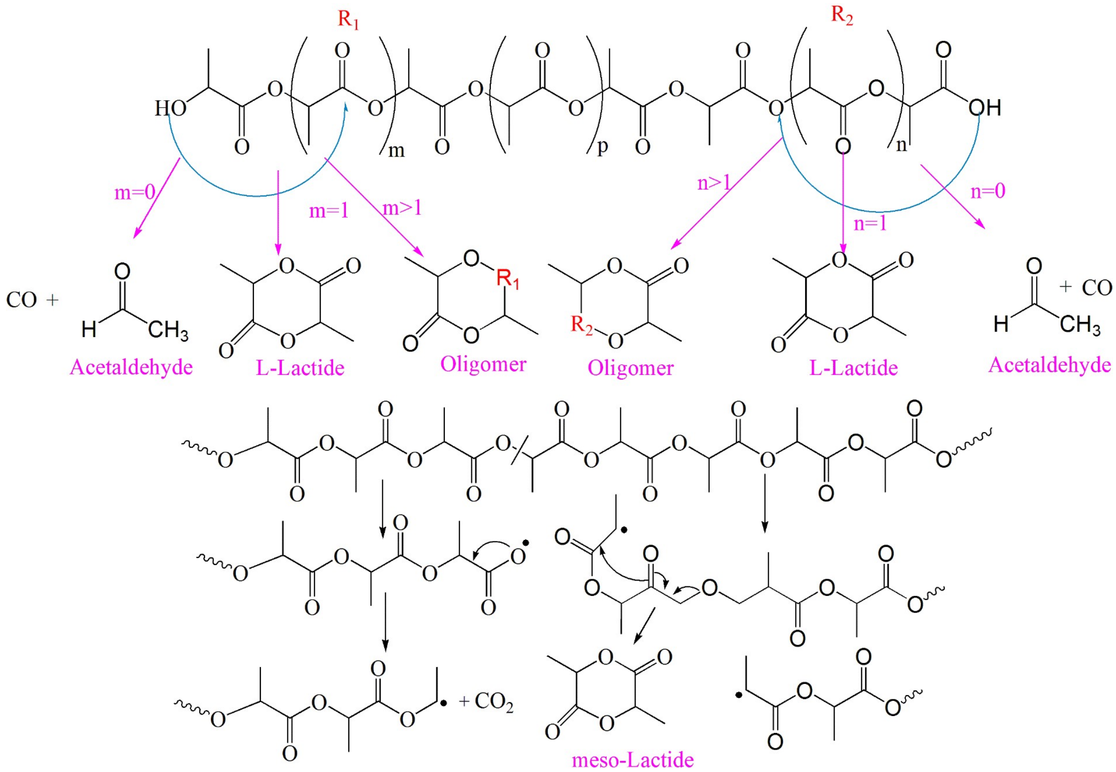

Fig. S2 Decomposition mechanism diagram of polylactic acid.

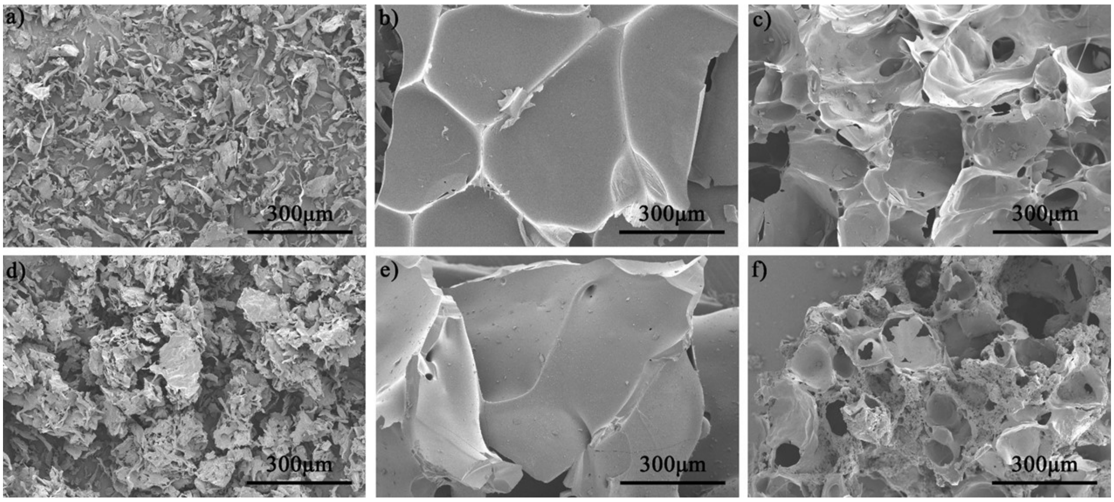

Fig. S3 The SEM of biochar (a) cellulose, (b) hemicellulose, (c) lignin, (d) cellulose/PLA, (e) hemicellulose/PLA, (f) lignin/PLA after pyrolysis

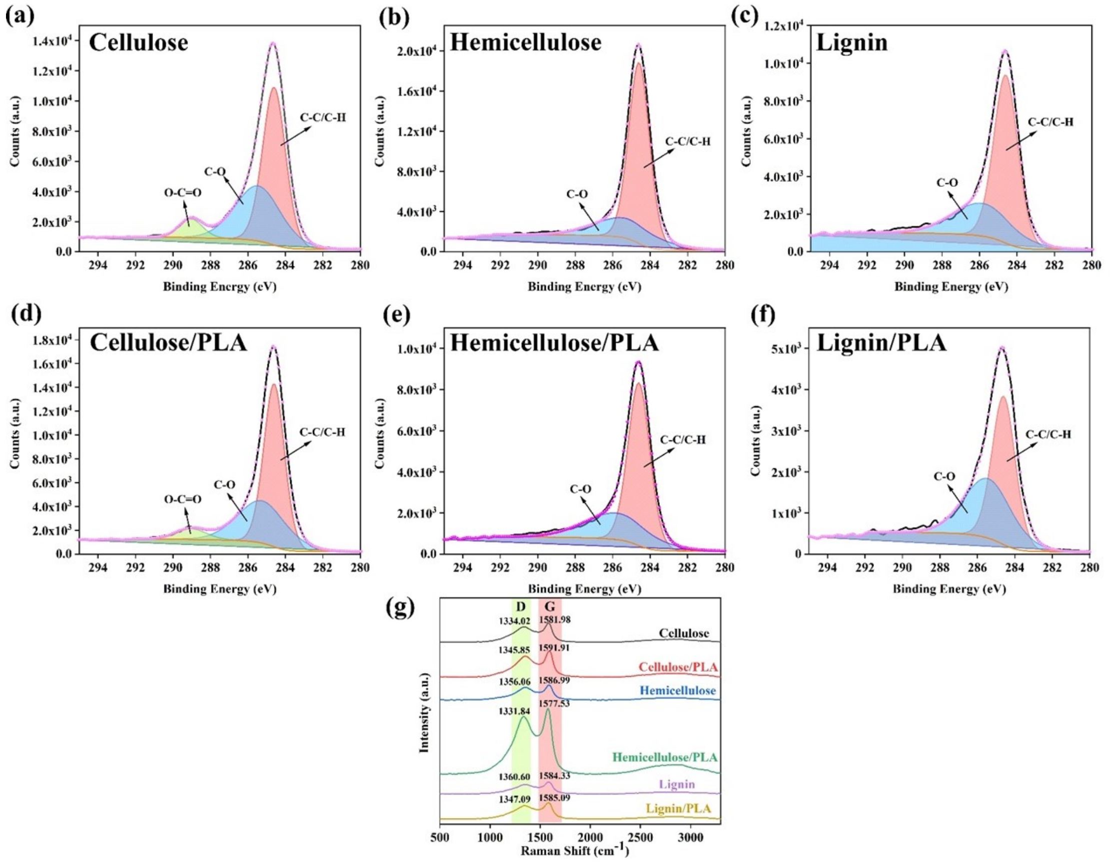

Fig. S4 The XPS analysis of (a) cellulose, (b) hemicellulose, (c) lignin, (d) cellulose/PLA, (e) hemicellulose/PLA, (f) lignin/PLA biochar after co-pyrolysis, (g) Raman spectrometer of biochar after co-pyrolysis

Table S2 Parameters for biochar after co-pyrolysis by XPS and Roman using peak area

	I_D/I_G	C	O	C-C	C-O	C=O
Cellulose	2.82	86.09	13.91	54.90	38.44	6.65
cellulose/PLA	2.72	90.01	9.99	58.65	35.55	5.80
Hemicellulose	2.56	94.85	5.15	75.45	24.55	-
hemicellulose/PLA	2.84	90.5	9.50	67.83	32.17	-
Lignin	2.86	93.86	6.14	67.52	32.48	-
lignin/PLA	3.06	91.18	8.82	54.65	45.35	-

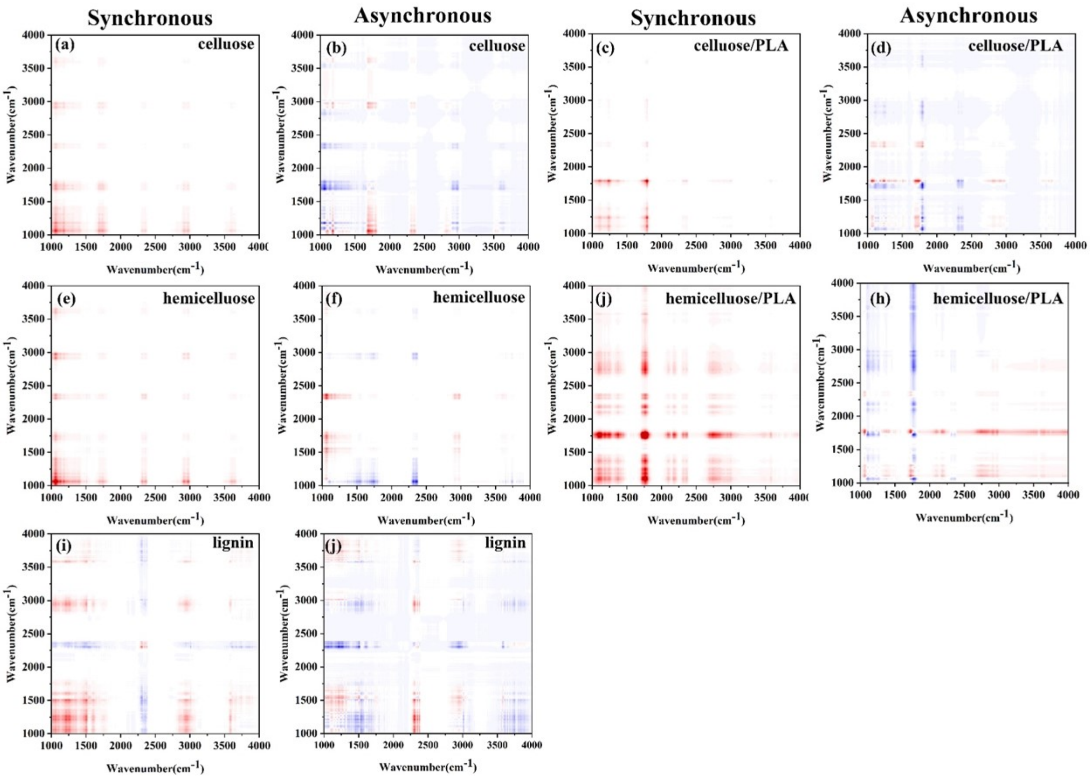

Fig. S5 The synchronous map of (a) cellulose, (c) cellulose/PLA, (e) hemicellulose, (j) hemicellulose/PLA (i) lignin; and the asynchronous map of (b) cellulose, (d) cellulose/PLA, (f) hemicellulose, (g) hemicellulose/PLA (h) lignin.

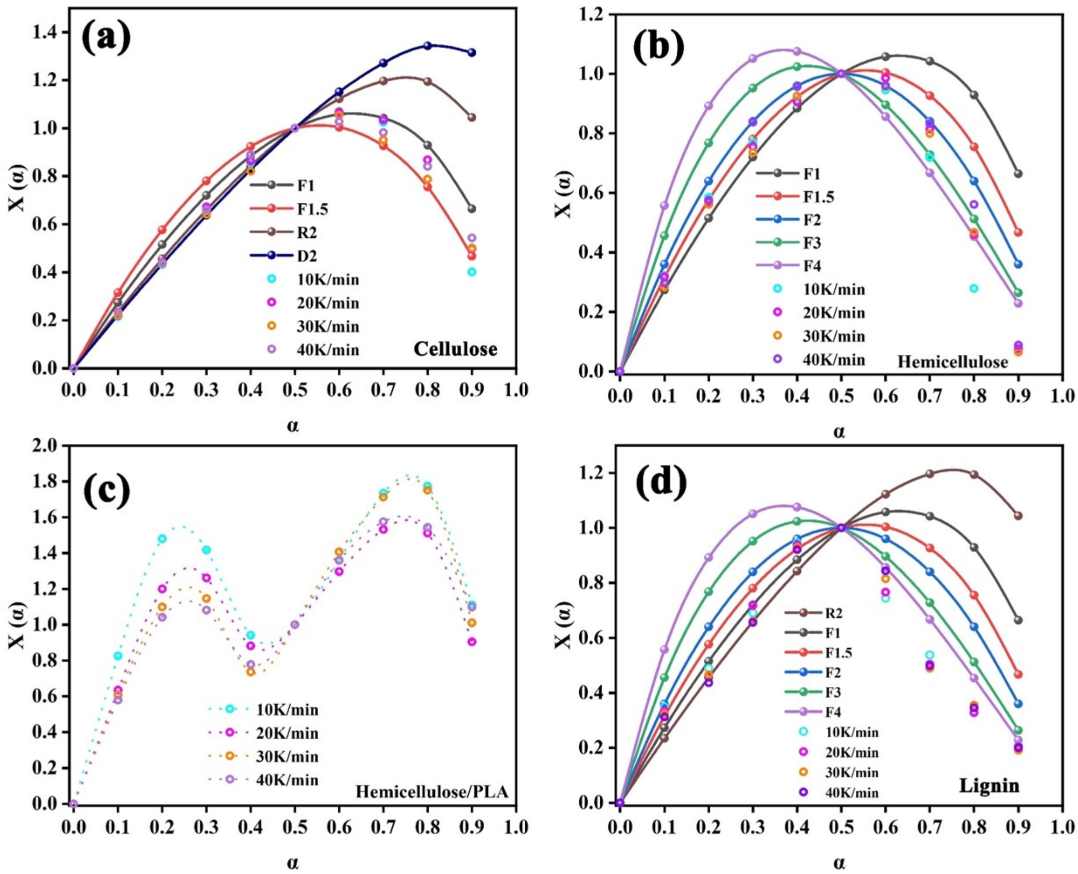

Fig. S6 The fitting curves of Criado method. (a) cellulose, (b) hemicellulose, (c) lignin, (d) hemicellulose/PLA